

A Bootstrap Method for Goodness of Fit and Model Selection with a Single Observed Network

Sixing Chen¹ and Jukka-Pekka Onnela¹

¹Department of Biostatistics, Harvard T.H. Chan School of Public Health, Boston, MA
sixingchen@hsph.harvard.edu, onnela@hsph.harvard.edu

Abstract

Network models are applied in numerous domains where data can be represented as a system of interactions among pairs of actors. While both statistical and mechanistic network models are increasingly capable of capturing various dependencies amongst these actors, these dependencies imply the lack of independence. This poses statistical challenges for analyzing such data, especially when there is only a single observed network, and often leads to intractable likelihoods regardless of the modeling paradigm, which limit the application of existing statistical methods for networks. We explore a subsampling bootstrap procedure to serve as the basis for goodness of fit and model selection with a single observed network that circumvents the intractability of such likelihoods. Our approach is based on flexible resampling distributions formed from the single observed network, allowing for finer and higher dimensional comparisons than simply point estimates of quantities of interest. We include worked examples for model selection, with simulation, and assessment of goodness of fit, with duplication-divergence model fits for yeast (*S.cerevisiae*) protein-protein interaction data from the literature. The proposed procedure produces a flexible resampling distribution that can be based on any statistics of one's choosing and can be employed regardless of choice of model.

Keywords single empirical network, network models, resampling, model selection, goodness of fit

1 Intro

Networks are well-suited to represent the structure of data from systems composed of interactions between pairs of actors (represented by nodes) that make up the system (Newman, 2010; Wasserman and Faust, 1994; Pastor-Satorras and Vespignani, 2007; Lusher et al., 2013; Raval and Ray, 2013). Often in such systems, these interactions (represented by edges) can depend on the state of the rest of the system, such as existing edges as well as attributes of nodes. One prominent example of this is triadic closure in social networks, where two people are more likely to become friends should they share a mutual friend (Watts, 2004). While innovations in network models are increasing the capability to encompass various dependencies between edges in the data, this rich level of interconnectedness poses a problem for statistical methods for networks.

In typical statistical settings, the premise is that the data is composed of independent observations. Typical methods are able to derive efficiency gains and consistency from a large number of samples due to this independence. However, in the network context where the structure of the network is of primary interest, the edges and their placement can be seen as the outcome, but there are often multiple layers of between-edge dependence. Thus, the premise of independent observations may not be met and most available statistical methods are therefore not applicable.

To see how limited statistical methods are for networks, one can inspect two prominent paradigms of network models. Statistical models are probabilistic models that specify the likelihood of observing any given network (Robins et al., 2007; Hoff et al., 2002; Goyal et al., 2014). One example is the family of exponential random graph models (ERGMs) (Lusher et al., 2013), which use observable configurations (such as triangles and k -stars) as the natural sufficient statistics. Although popular in practice, ERGMs can be difficult to fit and to sample from, and related methods may not scale well with large networks (An, 2016). Estimation for ERGMs can proceed via maximum pseudolikelihood estimation (MPLE) (Besag, 1974) or Markov chain Monte Carlo maximum likelihood estimation (MCMC-MLE) (Geyer and Thompson, 1992; Snijders, 2002). Pseudolikelihood methods for inference in ERGMs can lead to biased results due to the ignored dependence (Van Duijn et al., 2009), while inference for MCMC-MLE proceeds via simulation from estimated model (Snijders, 2002), and is thus entirely model based. On the other hand, mechanistic models are composed of generative mechanisms that prescribe the growth and evolution of a network over time (Barabási and Albert, 1999; Watts and Strogatz, 1998; Solé et al., 2002; Vázquez et al., 2003; Klemm and Eguiluz, 2002; Kumpula et al., 2007). While they are easy to sample from, a mechanistic model allows for numerous paths that can be taken in the state space to produce any one observed network, making the likelihood of all but the most trivial models intractable for networks of modest size. As a result, performing statistical procedures is difficult for such models and have little extant work in the literature.

In situations where likelihood based methods are not available, one often resorts to resampling methods, such as bootstrap, jackknife, and permutation tests (Efron, 1981; Good, 2006; Wu, 1986). Although the different resampling methods operate differently, they all serve to create new data sets from a single observed data set that mimic the behavior of the original one to serve as a basis for statistical procedures. This can be an attractive option for networks, since the data set can often consist of a single observed network. Examples include the internet and the world wide web, large social networks, certain biological networks, as well as transportation and infrastructural networks, to name a few. Having multiple resampled networks that resemble, in some ways, the original observed network can allow one to bypass dealing with the unwieldy likelihoods of current network models. Even in the best case, despite the likelihood having a simple functional form, the normalizing constants of ERGMs are generally unobtainable, since they require summing over an astronomical number of possible network realizations even for a network of modest size. In this paper, we will explore using a resampling procedure as a basis for statistical procedures for a single observed network.

There is some existing research on resampling methods in settings involving networks. First, there are methods for assessing the goodness of fit for a fitted model (Hunter et al., 2008; Shore and Lubin, 2015). These methods generally work by drawing network realizations from the fitted model, then assessing fit by comparing the value of a set of statistics for the observed network to the distribution of said statistics of the generated draws. This resampling scheme is akin to that of the parametric bootstrap. Note that this can be done for the point estimate of individual statistics or those of multiple statistics simultaneously, e.g., functionals of the degree distribution. However, the resamples in these methods are only representative of the fitted model and not necessarily of the observed network, and comparisons are made based only on point estimates. Second, there are methods for a setting where there are multiple independent networks observed

for MPLE (Desmarais and Cranmer, 2012). This is similar to the typical statistical setting with multiple independent observations and not applicable to the setting with just one observed network. Lastly, there are resampling methods based on subgraphs of subsamples of nodes in the observed network (Ohara et al., 2014; Bhattacharyya et al., 2015; Ali et al., 2016; Thompson et al., 2016; Gel et al., 2017). Ohara et al. (2014), Bhattacharyya et al. (2015), Thompson et al. (2016), and Gel et al. (2017) are aimed at estimation and uncertainty quantification of network centrality, distribution of subgraphs, and functionals of the degree distribution, while Ali et al. (2016) is a subgraph-based method for comparison between networks.

The procedure we propose makes use of the bootstrap subsampling scheme from Bhattacharyya et al. (2015). Our proposed bootstrap method addresses goodness of fit and model selection rather than estimation, and is based on the resampling distribution (rather than point estimates) of any set of statistics obtained from the induced subgraphs. The flexible choice of statistics allows an investigator to focus the criterion for model fit based on the aspects of the network of scientific interest. The flexibility of the full resampling distribution contains more information than simply aggregated subgraph counts and point estimates for comparison with candidate models. It also allows for natural uncertainty quantification regardless of the algorithm used for selecting the model. The proposed procedure is agnostic to the modeling paradigm (statistical or mechanistic) and can accommodate any model from which one can sample from, while providing very interpretable results. The scaling of the procedure depends on that of the statistics chosen as well as the number of subsamples taken. The latter is the only component native to our procedure and is linear.

The rest of the paper is organized as the following. In sections 2 through 4, we explain the proposed bootstrap subsampling procedure in detail, and highlight important considerations for some of the steps. In section 5, we elaborate on potential scenarios for when the proposed procedure could be used, and some of these are showcased with simulations and data example in section 6. Lastly, we conclude with discussions in section 7.

2 Subsampling Scheme and Resampling Distributions

Each subsample of the bootstrap subsampling scheme of Bhattacharyya et al. (2015) consists of a uniform node-wise subsample of all the nodes in the observed network G_o (with node set V_o and edge set E_o) and their induced subgraph, i.e., the nodes in the subsample and all edges between these nodes. For each subsample, one may compute any set of statistics to form a resampling distribution of these statistics. Although the subsamples will not be representative of a network the same size as the subsample from the true data generating mechanism, they will still retain features of the true data generating mechanism since the subsampling does not directly change any between-edge and between-node dependence that influenced the formation of the network, despite adding a degree of “missingness” by removing elements correlated with those in the subsample. In comparison, should one generate draws from a particular fitted model in order to form a resampling distribution, then the between-edge and between-node dependence will be those specified by the fitted model. In this case, the generated networks will only be representative of the true data generating mechanism if the fitted model is the true model, which is a strong assumption in most cases, and usually not verifiable in practice.

Due to each subsample only consisting of a subsample of V_o and E_o , each subsample will be missing elements that are correlated with those that are included in the subsample. As a result, this must be taken into account when any comparisons are made with a null/candidate model M_c . One may be tempted to compare subsamples of G_o with draws from M_c of the same size as the subsample. This should however be avoided since there is a degree of “missingness” in the subsamples of G_o that are not present in such draws from M_c . Even if M_c was the true model, this disparity could make the two behave differently. Instead, one should generate draws from M_c the same size as G_o and then apply the same subsampling to these draws. This way, both the subsamples of G_o and those of M_c will display the same amount of “missingness” and will be comparable. Should M_c be representative of the true data generating mechanism, then behavior of the two subsamples and the resampling distributions of computed statistics should be similar. The representativeness of the subsamples from G_o , as well as this comparability with the subsamples from M_c , form the basis for our statistical procedures. Even though we only consider uniform subsampling in the paper, the method for subsampling is flexible and can be chosen so that it is representative of sampling in practice or for statistical and computational ease. The proposed bootstrap subsampling procedure is summarized in **Figure 1**.

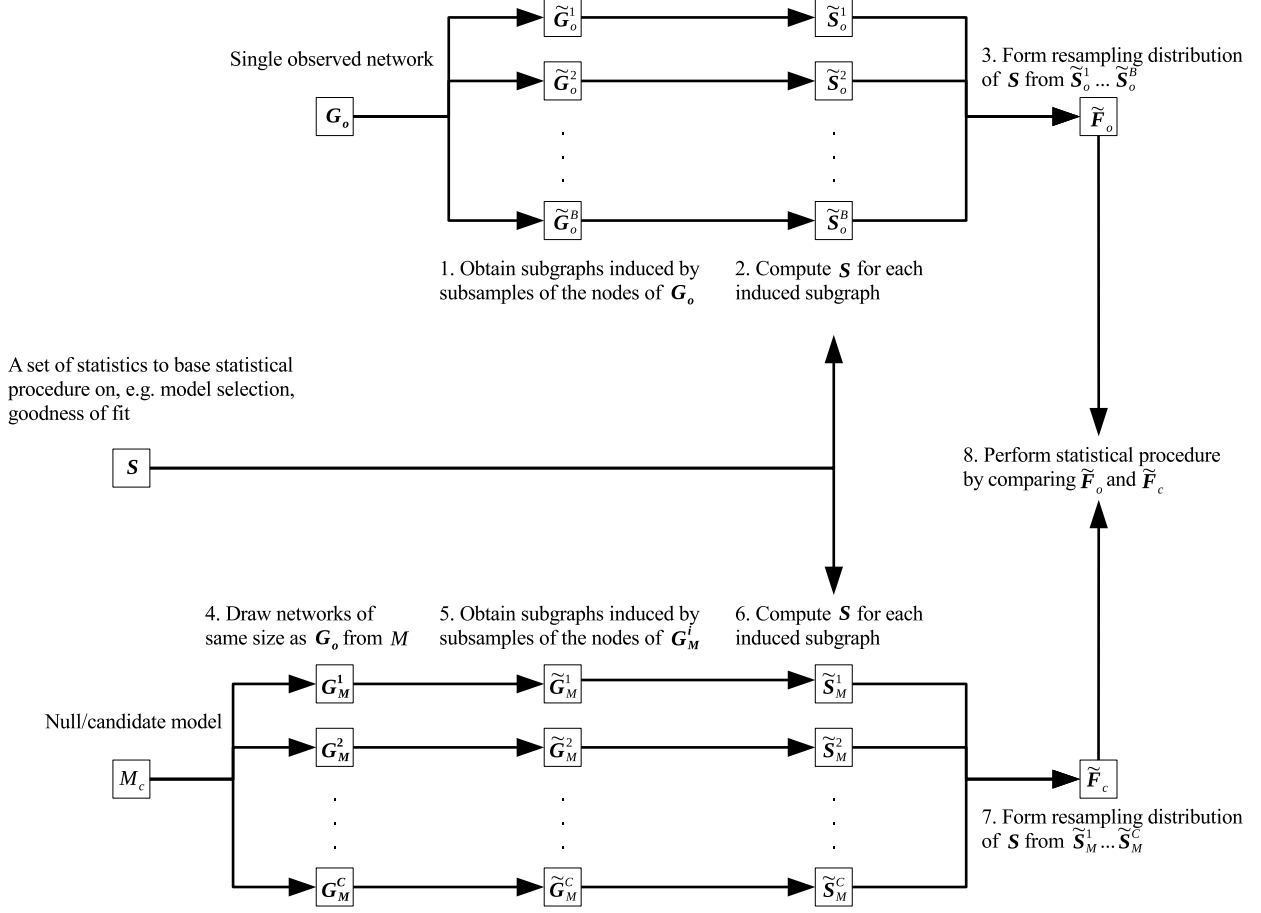


Figure 1: Schematic of the steps of the proposed bootstrap subsampling procedure for a single observed network G_o .

In contrast to existing methods that also use draws from the fitted model to assess goodness of fit, this approach can lead to a richer level of comparison. For existing methods, after choosing the statistics desired for assessing goodness of fit, the given statistics are computed for G_o and a large number of draws from M_c . The point estimate of these statistics for G_o are placed within the distribution of said statistics of the draws from M_c . Goodness of fit is then assessed by the location of the point estimate from G_o within the draws from M_c . This can be done visually or by quantifying the proportion of the draws with values of the statistics deemed more extreme. With our approach, the two resampling distributions can be compared on multiple levels, such as their location, spread, and shape. In addition, one can quantify the distance between the two with statistics such as the Kolmogorov-Smirnov (KS) statistic or the Kullback-Leibler divergence to order the fit of different candidate models.

One point of interest is that the subsamples from G_o are all from a single network, while subsamples from M_c are subsamples of independent networks drawn from M_c instead of subsamples from a single network drawn from M_c . The former is proposed due to potential instability of single generated networks and the corresponding subsamples, since there can be a great deal of instability in the generated networks depending on the model and the seed network used (often required to grow networks specified by mechanistic models). In addition, the disparity between the two styles of subsamples may depend on the proportion of the nodes in each subsample. Both of these points are further examined in the next two sections.

3 Stability under Sampling

When sampling from the candidate model, one needs to take care so the draws actually behave like the observed network even if the candidate model is the true model or is an accurate model, and in turn, the subsamples of these draws behave like the subsamples of the observed network. Such draws can look nothing like the observed network despite having a good candidate model, e.g., the draws having highly varying degree distributions that look nothing like that of the observed network. This issue can be more prominently demonstrated in the context of some mechanistic network models.

Networks generated from mechanistic models are often grown from a small (relative to the final size of the network) seed network according to the model’s generative mechanism until some stopping condition is reached, e.g. attaining a requisite number of nodes. There has works that show the original seed network has no influence on the degree distribution in the limit, i.e., for a large number of nodes, for certain types of mechanistic network models (Cooper and Frieze, 2003; Li et al., 2013). While some data sets, such as social networks, may be sufficiently large to reach this asymptotic regime, others, such as protein-protein interaction networks, may not be. Thus, when generating draws from candidate models for analysis of smaller networks, the original seed network can potentially have a great deal of influence. The seed network maybe as simple as a single node, or a complete graph of only three nodes, up to bigger complete graphs, or something more elaborate with more than one component. We briefly examine the effect of the seed network on the stability of the degree distribution of networks generated from the Erdős-Rényi and duplication-divergence models, of protein-protein interaction networks.

3.1 Erdős-Rényi Model

The Erdős-Rényi (ER) model (Erdős and Rényi, 1959) is a simple but rather unique model in that it can be framed as both a mechanistic and a statistical model. In the ER model, the number of nodes n is fixed, but there are two variants of the model that determine how the edges are placed. In the first variant, the $G(n, p)$ model, each of the $C(n, 2)$, n choose 2, possible edges are independent and are included in the graph with probability p , so the number of edges in the graph is binomial. In the other variant, the $G(n, m)$ model, the number of edges in the graph m is also fixed. In this case, the random graph has a uniform distribution over all $C(C(n, 2), m)$ possible graphs with n nodes and m edges.

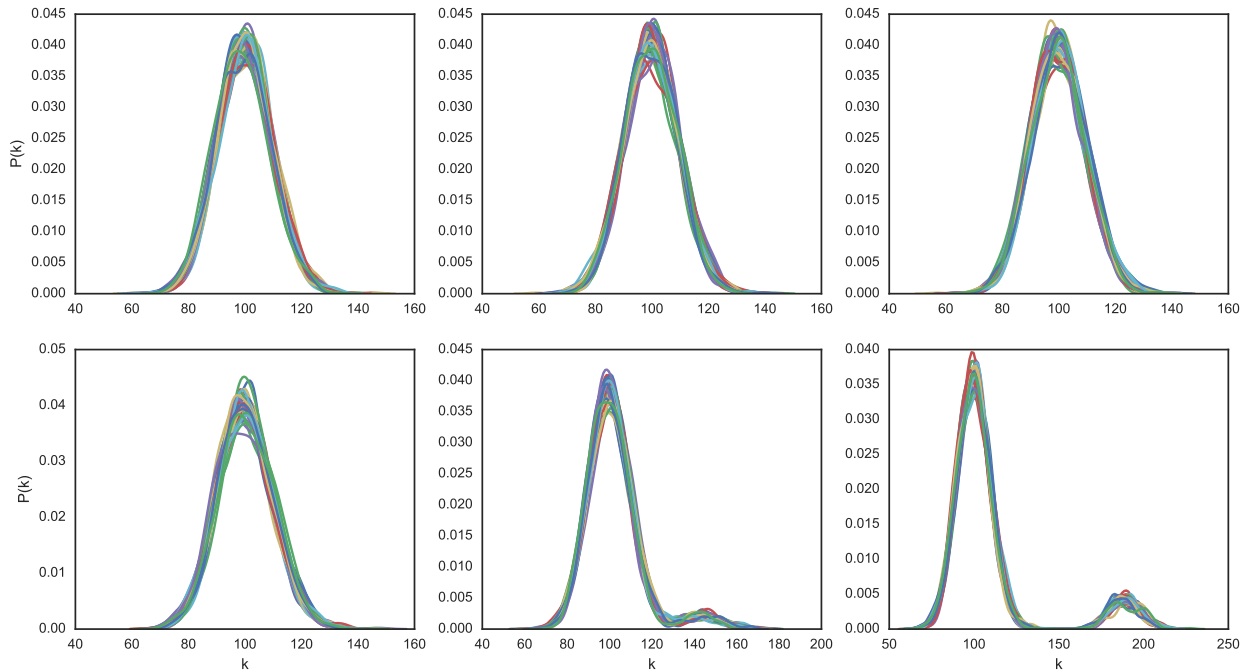


Figure 2: The degree distribution of 50 generated graphs from the $G(n = 1000, p = 0.1)$ model with seeds of 5, 8, 10, 20, 50, 100 nodes, from left to right, then top to bottom, as described in text.

The first variant can be easily framed as a mechanistic model. The network generation starts with a seed network of a single node. Then at each stage, a new node is added, and an edge between the new node and each existing node is added with probability p . This is done until there are n nodes in the network. Rather than starting with a seed network of a single node, networks can be generated according to the generative mechanism of the $G(n, p)$ model initialized with a different seed network. Here, we generated $G(n = 1000, p = 0.1)$ networks according to these rules, with complete graphs of 5, 8, 10, 20, 50, 100 nodes as the seed networks. We generated 50 networks of each size of the seed to evaluate the influence of the seed network on the stability of the degree distribution of the fully grown network.

The degree distribution of the 50 generated graphs at each size of the seed network are plotted in **Figure 2**. While the shape of the degree distribution understandably changes as the complete graph used as the seed network gets bigger, the size of the seed network seems to have little influence on the stability of the degree distribution. All 50 networks, for each size of the seed network, have very similar degree distributions. The width of the “band” of the 50 distributions stacked on top of one another also looks to be mostly unchanging. This seems to indicate that the variability in the degree distribution is largely unaffected by the size of the seed network.

3.2 Duplication-Divergence Models

Duplication-divergence models are a popular class of models used for protein-protein interaction networks. Examples include the duplication-mutation-complementation (DMC) (Vázquez et al., 2003) and duplication-mutation-random mutation models (DMR) (Solé et al., 2002; Pastor-Satorras et al., 2003). Given a seed network, both DMC and DMR models grow the network according to their respective generative mechanisms until the requisite number of nodes, n , is reached. In both the DMC and DMR models, a new node is first added at the beginning of each time step in network generation. An existing node is chosen uniformly at random for duplication, and an edge is then added between the new node and each neighbor of the chosen node. After this, the two models diverge. For DMC, for each neighbor of the chosen node, either the edge between the chosen node and the neighbor or the edge between the new node and the neighbor is removed with probability q_{mod} . The step is concluded by adding an edge between the chosen node and the new node with probability q_{con} . For DMR, each edge connected to the new node is removed with probability q_{del} . The step concludes by adding an edge between the new node and any existing node at the start of time step t with probability $q_{new}/n(t)$, where $n(t)$ is the number of nodes in the network at the start of time step t .

To assess stability of the degree distribution, we generated 50 network realizations of 1000, 3000, 5000, 7000, 10000 nodes from both models with the seed network set as a complete graph with 5, 8, 10, 20, 50, 100 nodes. The parameters of the DMC model were set as $q_{mod} = 0.2$ and $q_{con} = 0.1$, while those of the DMR model were $q_{del} = 0.2$ and $q_{new} = 0.1$. The degree distribution for the 50 generated networks at each combination of the size of the seed network and the total number of nodes for both models are plotted in **Figures 3 and 4**. A general trend in the plots is that the total number of nodes in the network has little to no influence on the stability of the degree distribution, while the size of the seed network has a great deal of influence, with stability increasing sharply with the size of the seed network, up to 50. For smaller seed networks, i.e., 3 or 5, the shape and spread of the degree distributions vary wildly even for larger networks. With a modest increase in the size of the seed network, i.e., 8 or 10, the shape and the spread of the degree distributions are more similar. Finally, for larger seed networks, i.e., 20, 50, or 100, the shape and spread of the degree distributions are quite uniform, and the width of the “band” of the 50 degree distributions stacked on top of one another also decreases. Clearly, the variability of the degree distribution depends greatly on the size of the seed network.

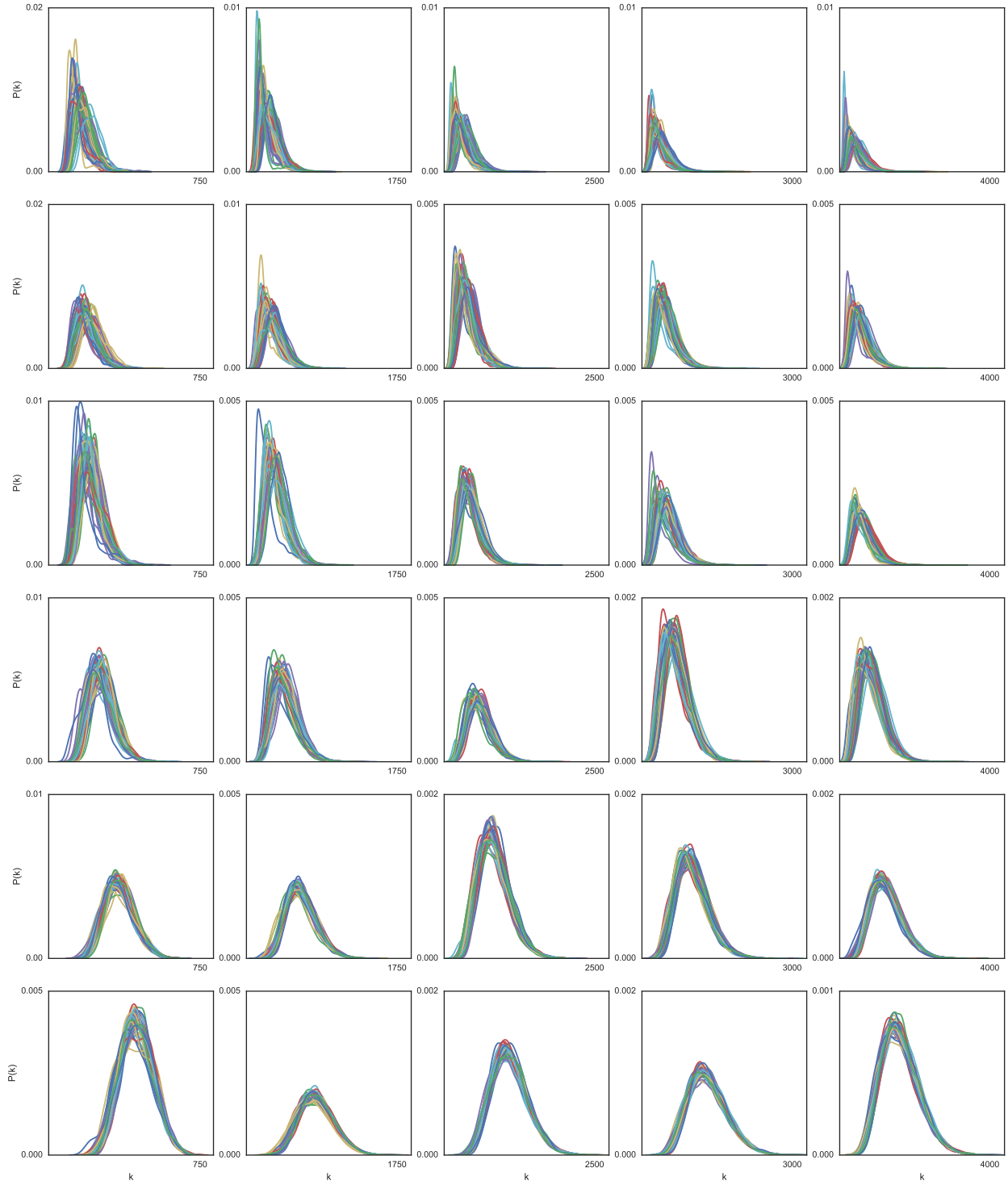


Figure 3: The degree distribution of 50 generated graphs of 1000, 3000, 5000, 7000, 10000 nodes from the DMC model, from left to right, with seeds of 5, 8, 10, 20, 50, 100 nodes, from top to bottom.

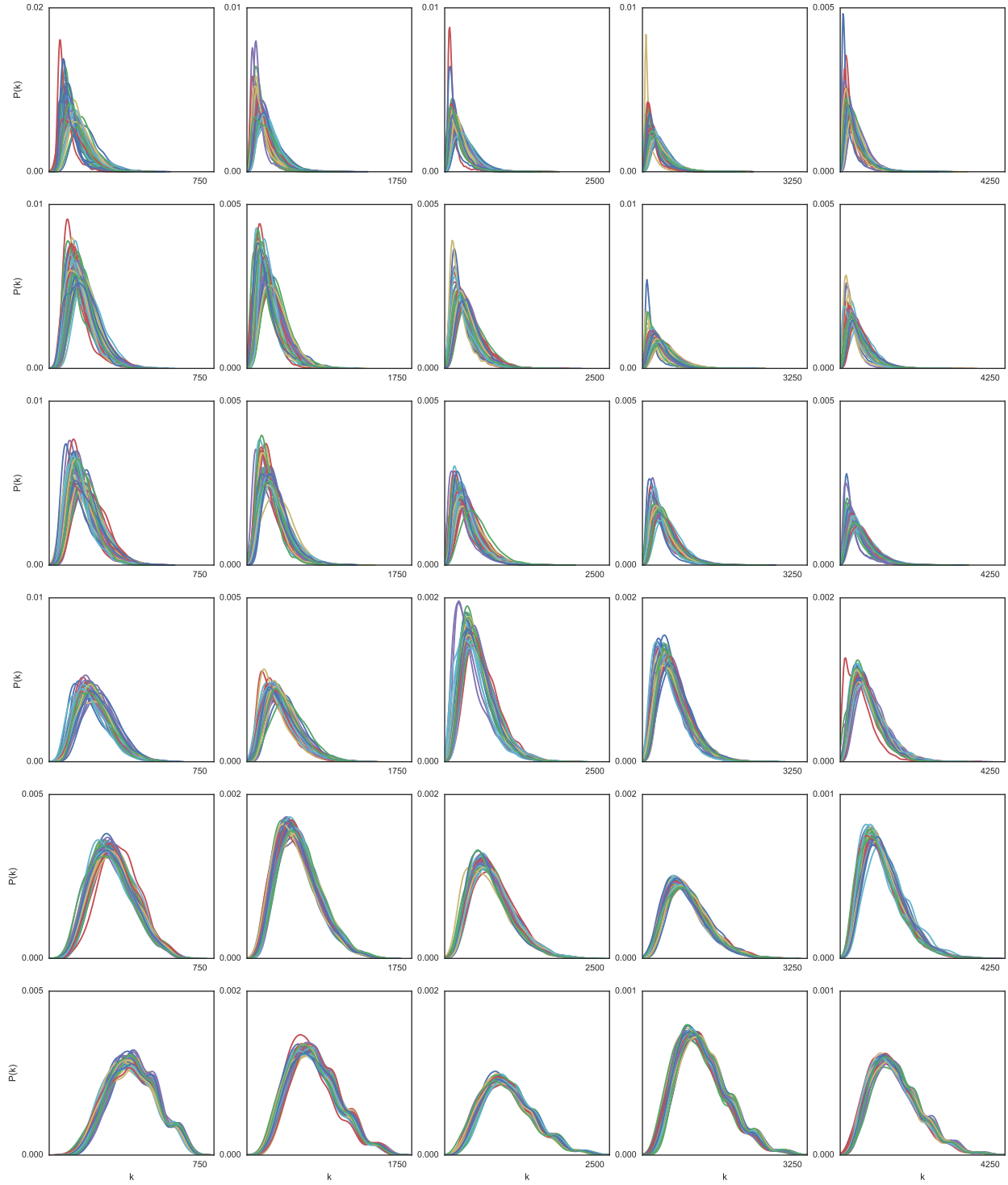


Figure 4: The degree distribution of 50 generated graphs of 1000, 3000, 5000, 7000, 10000 nodes from the DMR model, from left to right, with seeds of 5, 8, 10, 20, 50, 100 nodes, from top to bottom.

One big difference between the ER and DMC/DMR models is the dependence on existing edges on the formation of new ones. The instability in the degree distribution of networks generated from DMC/DMR models with small seed networks can be attributed to this dependence. While these two examples show the influence the seed network can potentially have in generating networks of modest size with mechanistic models, it does beg the question of how one selects a meaningful seed that leads to stable sampling while mimicking the behavior of the observed network in a principled way. Hypothetically, if the observed network is indeed generated from an ER model and assuming the seed network and the parameter values are well chosen, then the generated networks should mostly appear similar to the observed network due to the low variability regardless of the size of the seed. On the other hand, should the observed network come from a DMC/DMR model and assuming well chosen parameter values, as well as an appropriate but small seed network, then the generated networks are unlikely to appear similar to the observed network due to the high variability with small seeds as demonstrated.

4 Portion of Nodes to Include in Subsamples

The portion of nodes included in each subsample should not be so small such that no characteristics of the observed network or candidate models are retained, but also not so big such that the subsamples contain little variability. In one extreme, each subsample consists of just one node so that there is no structure within the induced subgraph, and in the other extreme, each subsample is simply the entire network. While the latter is of little concern when taking subsamples from independent draws from candidate models, it leaves no variability in the subsamples from a single observed network such that any resulting resampling distribution would simply be a point mass. What is an appropriate portion of nodes to include in each subsample?

Before attempting to answer this question, we define a criterion for performance in terms of the expectation of the KS statistic (lower values are better) between F_1 , the resampling distribution from the subsamples of a single network drawn from candidate model M_c , and F_c , that from subsamples of several independent networks drawn from M_c , where each subsample comes from different independent draws. This quantity is a measure of how closely F_o , the resampling distribution from the subsamples of the observed network, match F_c when the observed network is truly generated by M_c . If the KS statistic is small, discrepancy between F_o and F_c will be small if the model is correct. Additionally, this quantity being small implies that there is not much difference between using F_1 and F_c for comparison with F_o , thus we would be better off in electing for the stability of F_c . Note that the computation time required for F_c is greater than that for F_1 .

To compute the expectation of this KS statistic in general is not possible, since it largely depends on the network model and the seed network used. We will examine this quantity in the setting of the above mentioned $G(n, p)$ variant of the ER model, where the resampling distribution is the edge count in the induced subgraphs. We chose this model since the induced subgraph of an ER graph is once again an ER graph, so the distribution of the number of edges is still binomial and tractable.

The desired expectation of the KS statistic can then be written as follows, with a few approximations:

$$\begin{aligned}
E_G [\text{KS}(F_1(G), F_c)] &= \sum_g P(G = g) \text{KS}(F_1(g), F_c) \\
&= \sum_l \sum_{g: |E_g|=l} P(G = g) \text{KS}(F_1(g), F_c) \\
&\approx \sum_l \sum_{g: |E_g|=l} P(G = g) \text{KS}(\tilde{F}_1(l), F_c) \\
&= \sum_l \text{KS}(\tilde{F}_1(l), F_c) \sum_{g: |E_g|=l} P(G = g) \\
&= \sum_l \text{KS}(\tilde{F}_1(l), F_c) P(|E_G| = l)
\end{aligned}$$

The summation in the first line is over all the possible realizations, indexed by g , of a network G generated by the $G(n, p)$ model. Assuming the proportion of nodes in the subsample is α , then such an induced

subgraph of a network generated by the $G(n, p)$ model should be $G(\alpha n, p)$, since each of the possible edges of the induced subgraph are still independent and have a probability of p to exist. Thus, F_c would still be binomial, namely $B(C(\alpha n, 2), p)$, and remains constant. On the other hand, F_1 depends on g and is indicated as such. On the second line, a new index l , the number of edges in G , is introduced, with a nested summation for all g such that its edge set E_g has cardinality l . Next, we approximate $F_1(g)$ for g such that $|E_g| = l$ with $\tilde{F}_1(l)$, which only depends on l . Finally, we can write the nested summation on the fourth line as $P(|E_G| = l)$, the probability for G to have l edges.

Let $p_l = l/C(n, 2)$, then conditional on l , a randomly selected dyad (node pair) from the induced subgraph is an edge with probability p_l . Thus, one reasonable form for $\tilde{F}_1(l)$ would be $B(C(\alpha n, 2), p_l)$. We found this approximation to be accurate only when α is sufficiently small (< 0.3). For larger values of α , this approximation ignores the increasing effect of correlation between different subsamples due to increasing number of shared dyads, leading to underdispersion when using the $B(C(\alpha n, 2), p_l)$ approximation. To correct for the correlation, the covariance between two subsamples can be derived exactly, allowing for improved approximation of $\tilde{F}_1(l)$. Let EC_1 and EC_2 represent the node count from two different subsamples of m nodes from an ER graph of n nodes such that $|E_g| = l$. Then the covariance of EC_1 and EC_2 can be written as:

$$\text{cov}(EC_1, EC_2) = E[EC_1 \times EC_2] - E[EC_1] E[EC_2]$$

The form for $E[EC_i] = C(m, 2) \times p_l$ is simple, but the first term is more involved. Let $m^* = C(m, 2)$, $o^* = C(o, 2)$, e_j^i be the edge indicator for the j th dyad in the i th subsample, where \mathbb{O} s.t. $|\mathbb{O}| = o$ is the set of nodes that overlap between the two subsamples. Then the second term can be written as:

$$\begin{aligned} E[EC_1 \times EC_2] &= \sum_o E \left[\left(\sum_{j=1}^{m^*} e_j^1 \right) \left(\sum_{j=1}^{m^*} e_j^2 \right) \middle| |\mathbb{O}| = o \right] \times P(|\mathbb{O}| = o) \\ &= \sum_o A_o \times B_o \\ A_o &= o^* \times p_l + 2 \times C(o^*, 2) p_l^2 + 2(m^* - o^*) o^* p_l^2 + (m^* - o^*)^2 p_l^2 \\ B_o &\sim C(n, 2m - o) \times C(2m - o, o) \times C(2m - 2o, m - o) \end{aligned}$$

The detailed derivation for A_o and B_o are shown in the appendix. We also show in the appendix how to generalize the results to other models under dyadic independence, as well as for without dyadic independence.

Two pieces are needed to compute the last line of the expression for $E_G[\text{KS}(F_1(G), F_c)]$. $P(|E_G| = l)$ is simple to compute since G is $G(n, p)$, thus $|E_G|$ is distributed according to $B(C(n, 2), p)$. $\text{KS}(\tilde{F}_1(l), F_c)$ is less straightforward, but can be approximated using normal approximations. F_c can be approximated with a normal distribution with the corresponding binomial mean and variance, $N(C(\alpha n, 2)p, C(\alpha n, 2)p(1-p))$. For $\tilde{F}_1(l)$, the naive approximation that ignores correlation is similarly $N(C(\alpha n, 2)p_l, C(\alpha n, 2)p_l(1-p_l))$. However, as stated above, this approximation is inaccurate for larger values of α . We found that an approximation with a normal distribution with mean $C(\alpha n, 2)p_l$ and variance $E[EC_1^2] - E[EC_1]E[EC_2] - \text{cov}(EC_1, EC_2)$ yields a much closer approximation. Assume that $p \neq p_l$, then it can be easily verified that the maximal difference between the two normal CDFs occurs at x_l , the point where the two normal density functions are equal. Thus, for a particular value of l , $\text{KS}(\tilde{F}_1(l), F_c)$ can be approximated by the absolute value of the difference between the two normal CDFs evaluated at x_l .

α	0.05	0.1	0.15	0.2	0.25	0.3	0.5	0.6	0.7	0.8	0.9
$E_G[\text{KS}(F_1(G), F_c)]$ (naive)	0.0158	0.0317	0.0475	0.0633	0.0790	0.0947	0.1559	0.1855	0.2143	0.2422	0.2692
$E_G[\text{KS}(F_1(G), F_c)]$ (improved)	0.0158	0.0319	0.0482	0.0650	0.0821	0.0999	0.1792	0.2265	0.2824	0.3525	0.4517
$\hat{E}_G[\text{KS}(F_1(G), F_c)]$	0.0228	0.0383	0.0518	0.0690	0.0853	0.1033	0.1815	0.2284	0.2835	0.3532	0.4511

Table 1: Theoretical approximation and empirical estimate of $E_G[\text{KS}(F_1(G), F_c)]$ at various values of α , the proportion of nodes in each subsample.

Next, we examined the relationship between α and $E_G[\text{KS}(F_1(G), F_c)]$ in a numerical example. We computed $E_G[\text{KS}(F_1(G), F_c)]$, with the above approximations, for $n = 1000$, $p = 0.2$, and $\alpha \in \{0.05, 0.1,$

0.15, 0.2, 0.25, 0.3, 0.5, 0.6, 0.7, 0.8, 0.9}. In addition, we empirically estimated $E_G [\text{KS} (F_1 (G), F_c)]$ for each value of α via simulation, where $F_1 (g)$ is estimated from 10000 subsamples of each of 250 independent draws from $G (1000, 0.2)$ and F_c is estimated from single subsamples of 10000 independent draws from $G (1000, 0.2)$. The results are summarized in **Table 1**.

Clearly, $E_G [\text{KS} (F_1 (G), F_c)]$ increases with α , although not greatly in the lower range of values of α explored. The naive approximation matches the empirical results closely until about $\alpha = 0.3$, but is very inaccurate for larger values of α . The improved approximation matches the empirical results closely for all values of α and dominates the naive approximation for all values of α examined. The discrepancy between F_1 and F_c does increase with α , but remains small for reasonably small values of α . The improved approximation seems to adhere more closely to empirical results for larger values of α where more nodes are sampled. This is expected since the normal approximation for the binomial distribution improves with larger number of trials. Although this is merely a toy example and the results are by no means general, they do suggest to keep the portion of nodes in the subsample low ($< 30\%$ in this example) as long as sufficiently many features of the models can be retained. In addition, this is a cautionary tale about the care needed in choosing the proportion of nodes sampled, since even under dyadic independence, the difference between F_1 and F_c can be noticeably larger than an intuitive approximation for certain values of α .

5 Proposed Usage

There are a variety of statistical procedures that can take advantage of this sampling scheme, with a few of them detailed below. Before proposing the general framework for a few typical statistical procedures via the bootstrap subsampling procedure, we define the following notation for the rest of the section. The observed network will be referred to as G_o with B_o subsamples and corresponding induced subgraphs $\tilde{G}_o^{(1)} \dots \tilde{G}_o^{(B_o)}$. The draws from candidate model M_c will be referred to as $G_M^1 \dots G_M^{B_M}$ with corresponding subsample induced subgraphs $\tilde{G}_M^{(1)} \dots \tilde{G}_M^{(B_M)}$. Given a set of network statistics S chosen for model selection or assessing goodness of fit, the set computed from $\tilde{G}_o^{(1)} \dots \tilde{G}_o^{(B_o)}$ will be referred to as $\tilde{S}_o^{(1)} \dots \tilde{S}_o^{(B_o)}$, while those computed from $\tilde{G}_M^{(1)} \dots \tilde{G}_M^{(B_M)}$ will be referred to as $\tilde{S}_M^{(1)} \dots \tilde{S}_M^{(B_M)}$. Note that B_o and B_M need not be equal.

5.1 Model Selection

Suppose the goal is to select between candidate models $M_1 \dots M_c$ for G_o . Given a set of statistics S to base the model selection on, one needs to compute $\tilde{S}_{M_i}^{(1)} \dots \tilde{S}_{M_i}^{(B_{M_i})}$ from $\tilde{G}_{M_i}^{(1)} \dots \tilde{G}_{M_i}^{(B_{M_i})}$ for $i = 1 \dots c$. These collections of statistics along with the model indices of each draw form the training data and are the basis for the model selection procedure. The selection of S is flexible and should be chosen to prioritize the aspects of the network where similarity to the observed network is most paramount. The training data can be used to train any learning algorithm for prediction of the model index. Examples include random forest, support vector machine, or even ensemble learning algorithms like Super Learner (Polley et al., 2011; Van der Laan et al., 2007; Chen et al., 2018). Lastly, the trained algorithm can be evaluated at each of $\tilde{S}_o^{(1)} \dots \tilde{S}_o^{(B_o)}$ to give selected model $\hat{M}_1 \dots \hat{M}_{B_o}$, with majority rule deciding the final selected model.

Algorithm I: Steps for the model selection with the bootstrap subsampling procedure.

1. Draw subsamples $\tilde{G}_o^{(1)} \dots \tilde{G}_o^{(B_o)}$ from G_o
2. Draw subsamples $\tilde{G}_{M_i}^{(1)} \dots \tilde{G}_{M_i}^{(B_{M_i})}$ from each candidate model $i = 1 \dots c$
3. Compute statistics for model selection for $\tilde{G}_o^{(1)} \dots \tilde{G}_o^{(B_o)}$ and $\tilde{G}_{M_i}^{(1)} \dots \tilde{G}_{M_i}^{(B_{M_i})}$ for each $i = 1 \dots c$
4. Form training data based on each of $\tilde{S}_{M_i}^{(1)} \dots \tilde{S}_{M_i}^{(B_{M_i})}$ along with model index i
5. Train learning algorithm based on training data where the predictors are the network statistics and the outcome is the model index i
6. Evaluate trained algorithm on $\tilde{S}_o^{(1)} \dots \tilde{S}_o^{(B_o)}$ and select the model based on plurality rule

One distinct advantage of the model selection through this bootstrap subsampling procedure is that it gives inherent evidence about uncertainty or confidence in the selected model as well as other candidate models. The proportion of $\tilde{G}_o^{(1)} \dots \tilde{G}_o^{(B_o)}$ that are assigned to each model can be seen as evidence in favor of each candidate model, while the proportion of subsamples assigned the model that forms the majority can be seen as confidence in the selected model. With algorithms like random forest, where the decision is based on majority rule as well, this does not add anything new. But with others, such as support vector machine or the Super Learner that are not based on majority rule, this approach offers a way to quantify uncertainty without the need to alter the learning algorithm in any way.

5.2 Goodness of Fit

To assess the goodness of fit for candidate models $M_1 \dots M_c$, the procedure is similar to that of model selection. For a set of statistics S for assessing goodness of fit, one computes $\tilde{S}_o^{(1)} \dots \tilde{S}_o^{(B_o)}$ from $\tilde{G}_o^{(1)} \dots \tilde{G}_o^{(B_o)}$ and $\tilde{S}_{M_i}^{(1)} \dots \tilde{S}_{M_i}^{(B_M)}$ from $\tilde{G}_{M_i}^{(1)} \dots \tilde{G}_{M_i}^{(B_M)}$ for $i = 1 \dots c$. Rather than training a learning algorithm based on $\tilde{S}_{M_i}^{(1)} \dots \tilde{S}_{M_i}^{(B_M)}$ as in model selection, $\tilde{S}_o^{(1)} \dots \tilde{S}_o^{(B_o)}$ can be directly compared against $\tilde{S}_{M_i}^{(1)} \dots \tilde{S}_{M_i}^{(B_M)}$ for each i to assess fit. As mentioned above, this comparison between the distribution of $\tilde{S}_o^{(1)} \dots \tilde{S}_o^{(B_o)}$ and any set of $\tilde{S}_{M_i}^{(1)} \dots \tilde{S}_{M_i}^{(B_M)}$ can be done in terms of location, spread, shape, or other aspects of the distribution. This can be done visually by comparing the histograms of the two resampling distributions, but also numerically by comparing the mean and variance of the two.

Algorithm II: Steps for assessing goodness of fit with the bootstrap subsampling procedure.

1. Draw subsamples $\tilde{G}_o^{(1)} \dots \tilde{G}_o^{(B_o)}$ from G_o
2. Draw subsamples $\tilde{G}_{M_i}^{(1)} \dots \tilde{G}_{M_i}^{(B_M)}$ from each candidate model $i = 1 \dots c$
3. Compute $\tilde{S}_o^{(1)} \dots \tilde{S}_o^{(B_o)}$ and $\tilde{S}_{M_i}^{(1)} \dots \tilde{S}_{M_i}^{(B_M)}$ from $\tilde{G}_o^{(1)} \dots \tilde{G}_o^{(B_o)}$ and $\tilde{G}_{M_i}^{(1)} \dots \tilde{G}_{M_i}^{(B_M)}$, respectively
4. Assess fit by comparing $\tilde{S}_o^{(1)} \dots \tilde{S}_o^{(B_o)}$ and $\tilde{S}_{M_i}^{(1)} \dots \tilde{S}_{M_i}^{(B_M)}$

Assessment based on any one of these aspects may however lead to conflicting results, i.e., different models having the best fit depending on which aspect the comparison is based on, and it might be desirable to make comparisons through a more holistic measure. One solution to this is to compute a distance measure, such as the KS statistic or the Kullback-Leibler divergence, between $\tilde{S}_o^{(1)} \dots \tilde{S}_o^{(B_o)}$ and $\tilde{S}_{M_i}^{(1)} \dots \tilde{S}_{M_i}^{(B_M)}$ to quantify the fit of model i . This gives a single statistic that takes the entire distribution into account to quantify and to categorically order the fit of each candidate model. The KS test statistic and Kullback-Leibler divergence are typically computed in one dimension and can be used to compare the fit for each statistic individually as is. Instead, should one wish to make a comparison based on all statistics S at the same time, one can look to use generalizations of these statistics (Peacock, 1983; Fasano and Franceschini, 1987; Justel et al., 1997).

5.3 Comparison of Multiple Networks

If multiple networks are observed instead of a single network, and the goal is to assess how similar they are, then one can do so by building a resampling distribution from multiple networks. For the case of two observed networks with a set of statistics S for comparison and observed networks G_{o1} and G_{o2} , one can compute $\tilde{S}_{o1}^{(1)} \dots \tilde{S}_{o1}^{(B_{o1})}$ and $\tilde{S}_{o2}^{(1)} \dots \tilde{S}_{o2}^{(B_{o2})}$ from subsamples $\tilde{G}_{o1}^{(1)} \dots \tilde{G}_{o1}^{(B_{o1})}$ and $\tilde{G}_{o2}^{(1)} \dots \tilde{G}_{o2}^{(B_{o2})}$. The comparison of the two is based on $\tilde{S}_{o1}^{(1)} \dots \tilde{S}_{o1}^{(B_{o1})}$ and $\tilde{S}_{o2}^{(1)} \dots \tilde{S}_{o2}^{(B_{o2})}$, and one can proceed essentially the same way as with goodness of fit by comparing different aspects of the two distributions, but with $\tilde{S}_{o1}^{(1)} \dots \tilde{S}_{o1}^{(B_{o1})}$ and $\tilde{S}_{o2}^{(1)} \dots \tilde{S}_{o2}^{(B_{o2})}$ in place of $\tilde{S}_o^{(1)} \dots \tilde{S}_o^{(B_o)}$ and $\tilde{S}_{M_i}^{(1)} \dots \tilde{S}_{M_i}^{(B_M)}$. Should there be more than two observed networks for comparison, then the distance measure statistics can once again be used to quantify all pairwise relative similarities between the observed networks.

6 Simulation and Data Examples

We use a few simulation studies as well as data from an empirical network to illustrate the use of the bootstrap subsampling procedure in some of the scenarios described in the previous section.

6.1 Model Selection

The simulation studies conducted for model selection consider instances of a variation on the aforementioned $G(n, m)$ model we introduced (Chen et al., 2018). This variation generates random graphs with n nodes and m edges just as the $G(n, m)$ model with each edge being added one at a time. At each step in network generation, a pair of unconnected nodes are selected at random, and the probability for adding an edge between the two is determined based on the number of triangles it would close, then the edge is added with the given probability. This is repeated until there are m edges in the network. If the probability for adding an edge is fixed, then this is the $G(n, m)$ model. Instead, we start with a base probability p_0 to add the edge. Should the edge close at least one triangle, the probability increases by p_1 . Finally, should multiple triangles be closed by the edge, then the probability further increases by p_2 for each additional triangle closed.

In the simulation, we select between two instances of this model, both having $p_0 = 0.3$ and $p_1 = 0.1$. The difference comes in p_2 , with $p_2 = 0$ for model 1, while p_2 varies over 0.05, 0.03, 0.01, 0.005 for model 2. For given choices of n and m , as p_2 decreases and gets closer to 0, the difference between the two models become more difficult to detect. The generated networks consist of 100 nodes with edge count varying over 100, 500, 1000, 2000. For a given set of parameter values, the difference between the two models should be easier to detect as edge count increases, since attenuation from the difference in p_2 has more opportunities to manifest itself. The training data consists of a single subsample of 80 nodes for each of 10000 draws from each model ($\tilde{G}_{M_i}^{(1)} \dots \tilde{G}_{M_i}^{(10000)}$). The test data consists of 1000 draws from each model (G_o), while the model selection is based on 100 subsamples of 80 nodes from each draw ($\tilde{G}_o^{(1)} \dots \tilde{G}_o^{(100)}$).

The model selection is through the Super Learner (see citations in section 5.2 for details), with support vector machine, random forest, and k -nearest neighbors as candidate algorithms, and average clustering coefficient, triangle count, as well as the three quartiles of the degree distribution as predictors. These statistics were chosen as predictors since the difference in p_2 directly affects formation of triangles, while the other statistics are influenced strongly by triangles. For each of the 100 $\tilde{G}_o^{(b_o)}$ for a particular testing network G_o , the Super Learner will give a score between 0 and 1 for predicting the model class of $\tilde{G}_o^{(b_o)}$, with score < 0.5 assigned model 1 and score > 0.5 assigned model 2. The selected model is the model assigned to more $\tilde{G}_o^{(b_o)}$ s, i.e., the majority of model assignment.

The results of the simulation are summarized in **Figure 5** and **Table 2**. **Table 2** contains the proportion of test networks whose model was correctly classified by the Super Learner at each combination of p_2 and edge count. Unsurprisingly, the proportion decreases as p_2 decreases for a fixed edge count, and increases as edge count increases for a fixed p_2 . **Figure 5** shows the histogram of the confidence for the correct model. When model 1 is the true model of the test network, this is the proportion of the 100 subsamples that were assigned model 1, and vice versa. When the proportion of correctly classified models is around 0.5, i.e., as good as a random guess, the confidence is symmetric and centered close to 0.5. When the proportion is higher than 0.5, the distribution of the confidence is shifted to the right, meaning that the two models are easier to tell apart. In addition, the more right skewed the histograms, the more confidence in the correct model. The red vertical line indicates the median, which also moves to the right as the proportion increases and as the confidence becomes more right skewed. This behavior indicates that the confidence for the selected model from the bootstrap subsampling procedure quantifies well the degree of uncertainty in the selected model.

	$p_2 = 0.05$	0.03	0.01	0.005
Edge count = 100	0.5015	0.5005	0.4834	0.5100
500	0.6092	0.5670	0.5178	0.5076
1000	0.9203	0.8202	0.6249	0.5786
2000	0.9890	0.9740	0.8343	0.6810

Table 2: Proportion of the test networks correctly classified at each combination of p_2 and edge count.

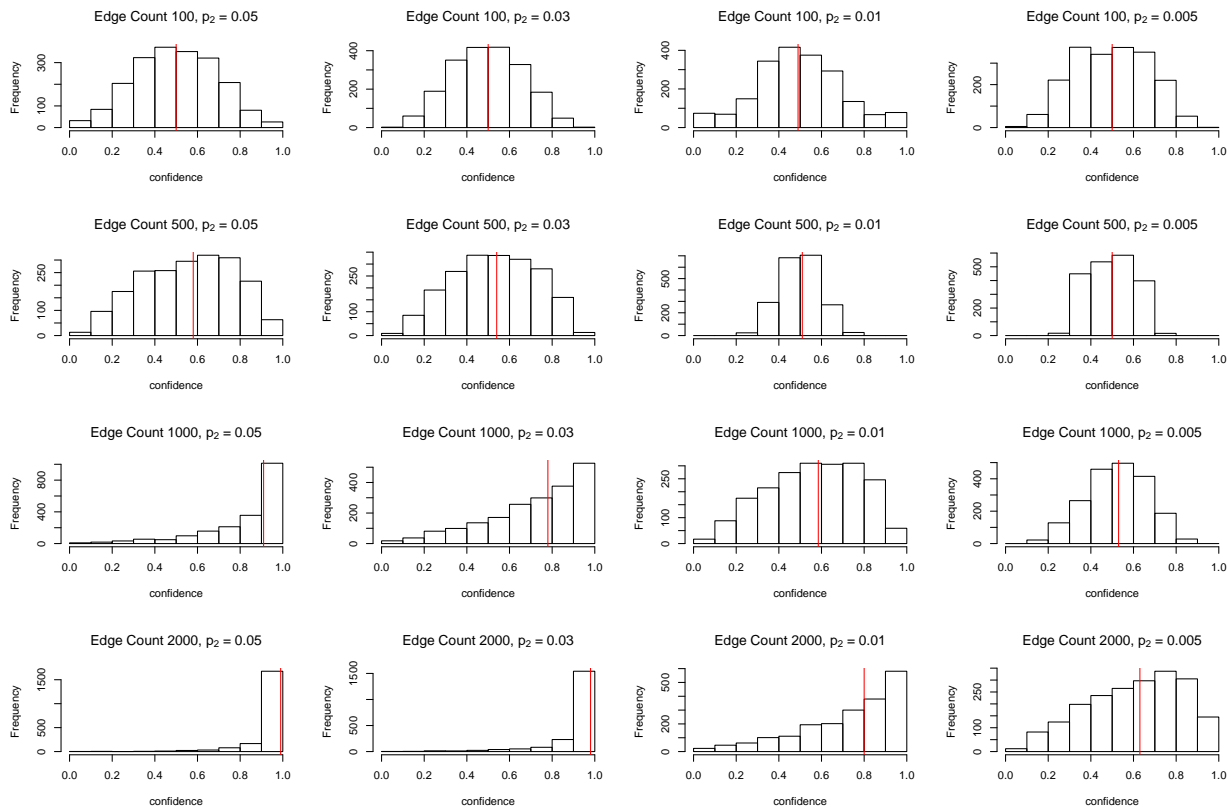


Figure 5: Histograms of the confidence score (proportion of subsamples assigned the correct model here rather than the majority) for p_2 from 0.05, 0.03, 0.01, 0.005, from left to right, and edge count from 100, 500, 1000, 2000, from top to bottom, with the red vertical lines representing the median.

6.2 Goodness of Fit

To display our method for assessment of goodness of fit, we examine the yeast (*S.cerevisiae*) protein-protein interaction network data from the database of interacting proteins (DIP) (Salwinski et al., 2004). This data set has been much examined in the literature, including via network models. There are two particular publications (Hormozdiari et al., 2007; Schweiger et al., 2011) that fit different duplication divergence models to two different previous versions of the yeast data set, with differing seed networks. Here we apply our method to compare the fit of the two different models on the most recent version of the data.

Both papers use the same duplication divergence model (Solé et al., 2002; Pastor-Satorras et al., 2003), which we described as DMR in section 3.2. However, the papers used different parameter values as well as different seed networks. The fit from Hormozdiari et al. (2007) has parameter values $p = 0.365$ and $r = 0.12$, and the seed network contains 50 nodes. The seed network¹ was constructed by highly connecting cliques, complete graphs where an edge exists between every pair of nodes, of 7 nodes and 10 nodes, then connecting additional nodes to the cliques. To highly connect the cliques, each possible edge between nodes in different cliques (70 such edges) was added with probability 0.67. Then, another 33 nodes were attached to randomly chosen nodes from the two cliques. At each step of the network generation, if a singleton (a node not connected to any other node) was generated, it was immediately removed in their model.

On the other hand, the fit from Schweiger et al. (2011) has parameter values $p = 0.3$ and $r = 1.05$. They use a smaller seed network of 40 nodes, generated with an inverse geometric model. To generate this seed network, a set of coordinates $\{x_1 \dots x_{40}\}$ in \mathbb{R}^d is generated for each node. Then, each pair of nodes with distance $\|x_i - x_j\|$ greater than some threshold R is connected with an edge. Each dimension of the

¹Note that the details for obtaining the seed network from Hormozdiari et al. (2007) was somewhat incomplete, so this is our interpretation of the description of their seed network.

coordinates is independently generated from the standard normal distribution $N(0, 1)$. In their fit, the seed network uses $d = 2$ and $R = 1.5$. Unlike Hormozdiari et al. (2007), Schweiger et al. (2011) does not remove singletons as they are generated.

Both papers assessed the fit of their model by comparing certain aspects of the generated network to those of the yeast PPI network. In Hormozdiari et al. (2007), the fit of their model was assessed via k -hop reachability, the number of distinct nodes reachable in $\leq k$ edges, the distribution of particular subgraphs, such as triangles and stars, as well as some measures of centrality. Schweiger et al. (2011) does so with the distribution of bicliques, i.e., subgraphs of two disjoint sets of nodes where every possible edge between the two sets exists. Here, we assess the fit of both models via our method with the average local clustering coefficient, triangle count, as well as the degree assortativity. The local clustering coefficient of a particular node is a measure of how much does its neighbors resemble a clique. Mathematically, this is computed as the number of edges between a node’s neighbors divided by the possible number of such edges. We use the average of the local clustering coefficient over all nodes in the network as a measure of local clustering that is also attributable to the network as a whole. We also consider the number of triangle subgraphs that appear in the network. Unlike Hormozdiari et al. (2007), which counts the total number of various subgraphs together, the count of triangles alone is a strictly global measure of clustering. Lastly, the degree assortativity of a network is a measure of how similar are the degrees of nodes connected by an edge. It is defined as the Pearson correlation of the degrees of nodes connected by an edge, so positively assorted networks have more edges between nodes of similar degrees, while negatively assorted networks have more edges between nodes of dissimilar degrees.

For the analysis, we consider the largest connected component (LCC) of the PPI network just as in Hormozdiari et al. (2007). The full network from the current version of the data contains 5176 nodes and 22977 edges, while the LCC contains 5106 (98.6%) nodes and 22935 (99.8%) edges. Networks drawn from each model contains the same number of nodes as the LCC, starting from their respective seed networks described above. Subsamples from the PPI network as well as networks drawn from each model contain 1550 nodes, roughly corresponding to 30%. This was the largest portion considered in section 4.

The results of the data analysis are summarized in **Figure 6**. From the figures, it’s clear that the ordering of the fit of both models differ based on the statistic of comparison. For clustering coefficient, both models fit equally poorly, as the resampling distribution of both models and that of the PPI network have no overlap at all. The KS statistic between the resampling distribution of the PPI network and that of each model are both 1, indicating very poor fit. The distance between the location of both models’ resampling distribution and that of the PPI network are very similar, so existing methods that assess goodness of fit based on point estimates only likely would arrive at the same conclusion. For triangle count, the model of Schweiger et al. (2011) seems to fit better as its resampling distribution’s spread has a much bigger overlap with that of the PPI network. The KS statistic for the model of Schweiger et al. (2011) (0.6778) is also much smaller than that of Hormozdiari et al. (2007) (0.9018). However, unlike clustering coefficient, the distance between the location of both models’ resampling distribution and that of the PPI network are rather similar, so existing methods likely would have concluded that the fit of both models are similar in this regard. Lastly, for degree assortativity, the model of Hormozdiari et al. (2007) fits much better as all of the spread of its resampling distribution overlaps with that of the PPI network, and most of its spread is negative just as the PPI network, indicating negative degree assortativity. On the other hand, the resampling distribution of the model of Schweiger et al. (2011) is entirely positive and has little overlap with that of the PPI network. The KS statistic tells the same story, with 0.4373 for Hormozdiari et al. (2007) and 0.9782 for Schweiger et al. (2011). The distance of the location of the two models’ resampling distributions to that of the PPI network are very distinct, so existing methods would likely reach the same conclusion. We can see situations in this data set where existing methods and our method would reach the same conclusion, but also where the two would reach different conclusions due to the additional layer of information encoded in the resampling distributions.

In addition in **Figure 6**, we plot the subsamples from two individual networks drawn from each model against the subsamples from independent networks drawn from each model. For each statistic, the spread and location of the two types of subsamples are similar. This is likely due to the rather large seeds (50 and 40 nodes respectively) both models use as well as the rather small portion of nodes in each subsample ($\sim 30\%$), reflecting observations from sections 3 and 4.

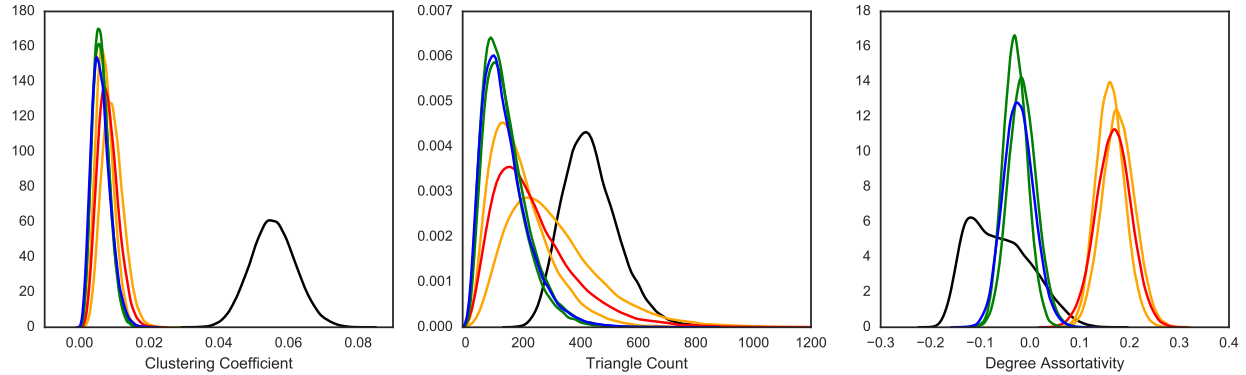


Figure 6: The resampling distribution of clustering coefficient, triangle count, and degree assortativity (left to right) from independent draws from the two model fits (blue for Hormozdiari et al. (2007) and red is for Schweiger et al. (2011)) as well as the PPI network (black). In addition, there are two resampling distributions from a single draw from each of the two model fits (green for Hormozdiari et al. (2007) and orange is for Schweiger et al. (2011)).

7 Discussion

Network models continue to expand the amount of correlation they can incorporate and are able to model increasingly complex dependencies that can arise in network data. Yet this very dependency poses a statistical challenge, especially in the case of a single observed network. We propose a bootstrap subsampling procedure as a basis for statistical procedures in this setting that is based on a flexible resampling distribution built from the single observed network.

Given any statistic of interest, its corresponding resampling distribution can be compared against its analog from a null/candidate model based on any attribute of their distributions, including, but not limited to, location, spread, shape, measures of mean, as well as distances. In comparison, existing methods in this setting typically rely on the point estimate from the observed network, which leads to a more limited comparison. As seen in our data example, this additional layer of information can sometimes lead to a different conclusion than existing methods. In addition, the distance between the resampling distributions leads to a single holistic measure for comparison as well as ordering of different network models.

The flexibility in our approach is not limited to what one can do with these resampling distributions, but also the type of subsampling used to generate them. Although in the simulation and data example, the subsamples are simply random samples of the nodes of the network, they need not always be. In fact, any method of subsampling is valid as long as it is applied to both the observed data and the null/candidate model. Thus, it can be tailored to any needs of the investigator, such as statistical or computational considerations. The method of subsampling can be also used as a sensitivity analysis to see whether the results of the analysis remain unchanged under different methods of subsampling. This consideration for different methods of subsampling motivates the most immediate step for future work as it begs the question whether they can lead to performance gains. Perhaps certain types of subsampling can outperform others given the method of sampling used to obtain the observed data.

Acknowledgements

S.C. and J.P.O. are both supported by NIH 1DP2MH103909-01. In addition, S.C. is supported by NIH 5U01HG009088-02 and U54GM088558-09; J.P.O is supported by NIH 5R37AI051164-12, 1R01AI112339-01, and U54GM088558-06.

Appendix

Following the uniform nodewise subsampling from the paper for the ER model. To better approximate the resampling distribution, we need to estimate the covariance between different subsamples of the same size from the same ER graph.

Say the full ER graph has n nodes, and each subsample contains m nodes. Let EC_1 and EC_2 represent the node count from two different subsamples of m nodes from an ER graph of n nodes containing $p_l \times C(n, 2)$ edges:

$$\text{cov}(EC_1, EC_2) = E[EC_1 \times EC_2] - E[EC_1] E[EC_2]$$

$E[EC_i] = C(m, 2) \times p_l$, so we need to focus on the first term. Let $m^* = C(m, 2)$, $o^* = C(o, 2)$, e_j^i be the edge indicator for the j th dyad in the i th subsample, and \mathbb{O} be the set of nodes that overlap between the two subsamples:

$$E[EC_1 \times EC_2] = \sum_o E \left[\left(\sum_{j=1}^{m^*} e_j^1 \right) \left(\sum_{j=1}^{m^*} e_j^2 \right) \middle| |\mathbb{O}| = o \right] \times P(|\mathbb{O}| = o) = \sum_o A_o \times B_o$$

We assess the two terms separately, say the first o^* dyads are from the nodes that overlap:

$$\begin{aligned} A_o &= E \left[\left(\sum_{j=1}^{m^*} e_j^1 \right) \left(\sum_{k=1}^{m^*} e_k^2 \right) \middle| |\mathbb{O}| = o \right] \\ &= E \left[\left(\sum_{j=1}^{o^*} e_j^1 + \sum_{j=o^*+1}^{m^*} e_j^1 \right) \left(\sum_{k=1}^{o^*} e_k^2 + \sum_{k=o^*+1}^{m^*} e_k^2 \right) \middle| |\mathbb{O}| = o \right] \\ &= E \left[\left(\sum_{j=1}^{o^*} e_j^1 \right) \left(\sum_{k=1}^{o^*} e_k^2 \right) + \left(\sum_{j=1}^{o^*} e_j^1 \right) \left(\sum_{k=o^*+1}^{m^*} e_k^2 \right) \right. \\ &\quad \left. + \left(\sum_{j=o^*+1}^{m^*} e_j^1 \right) \left(\sum_{k=1}^{o^*} e_k^2 \right) + \left(\sum_{j=o^*+1}^{m^*} e_j^1 \right) \left(\sum_{k=o^*+1}^{m^*} e_k^2 \right) \middle| |\mathbb{O}| = o \right] \\ &= \sum_{j=1}^{o^*} \sum_{k=1}^{o^*} E[e_j^1 e_k^2] + \sum_{j=1}^{o^*} \sum_{k=o^*+1}^{m^*} E[e_j^1 e_k^2] + \sum_{j=o^*+1}^{m^*} \sum_{k=1}^{o^*} E[e_j^1 e_k^2] + \sum_{j=o^*+1}^{m^*} \sum_{k=o^*+1}^{m^*} E[e_j^1 e_k^2] \\ &= \sum_{j=1}^{o^*} E[(e_j^1)^2] + \sum_{j \neq k \in \{1 \dots o^*\}} E[e_j^1] E[e_k^2] \\ &\quad + \sum_{j=1}^{o^*} \sum_{k=o^*+1}^{m^*} E[e_j^1] E[e_k^2] + \sum_{j=o^*+1}^{m^*} \sum_{k=1}^{o^*} E[e_j^1] E[e_k^2] + \sum_{j=o^*+1}^{m^*} \sum_{k=o^*+1}^{m^*} E[e_j^1] E[e_k^2] \\ &= \sum_{j=1}^{o^*} P(e_j^1 = 1) + 2 \sum_{j < k \in \{1 \dots o^*\}} P(e_j^1 = 1) P(e_k^2 = 1) + \sum_{j=1}^{o^*} \sum_{k=o^*+1}^{m^*} P(e_j^1 = 1) P(e_k^2 = 1) \\ &\quad + \sum_{j=o^*+1}^{m^*} \sum_{k=1}^{o^*} P(e_j^1 = 1) P(e_k^2 = 1) + \sum_{j=o^*+1}^{m^*} \sum_{k=o^*+1}^{m^*} P(e_j^1 = 1) P(e_k^2 = 1) \\ &= o^* \times p_l + 2 \times C(o^*, 2) p_l^2 + 2(m^* - o^*) o^* p_l^2 + (m^* - o^*)^2 p_l^2 \end{aligned}$$

In the fourth line, the last three terms are all from products of distinct dyads, so the expectation of the product can be separated into product of the expectation. The first term however does contain some products of the same dyad, and need to be handled differently. For the first term in the fourth line, since

the first o^* dyads are the same in the two subsamples:

$$\begin{aligned} \sum_{j=1}^{o^*} \sum_{k=1}^{o^*} E [e_j^1 e_k^2] &= \sum_{j=k \in \{1 \dots o^*\}} E [e_j^1 e_k^2] + \sum_{j \neq k \in \{1 \dots o^*\}} E [e_j^1] E [e_k^2] \\ &= \sum_{j=1}^{o^*} E [(e_j^1)^2] + \sum_{j \neq k \in \{1 \dots o^*\}} E [e_j^1] E [e_k^2] \end{aligned}$$

For B_o :

$$\begin{aligned} B_o &= P(|\mathcal{O}| = o) \\ &= \frac{\# \text{ of ways to choose two different subsets of } n \text{ elements that have } o \text{ overlapping elements}}{\# \text{ of ways to choose two different subsets of } n \text{ elements}} = \frac{B_o^1}{B_o^2} \end{aligned}$$

We need not compute the denominator, but merely normalize the numerator for all possible values of $o \in \{\max(0, 2m - n) \dots m\}$. Note that the union of the two subsets is a set of $2m - o$ elements

$$\begin{aligned} B_o^1 &= (\text{number of ways of choosing } 2m - o \text{ elements out of } n) \\ &\quad \times (\text{number of ways of choosing the } o \text{ overlapping elements out of } 2m - o) \\ &\quad \times (\text{number of ways to permute the nonoverlapping } 2m - 2o \text{ elements between the two subsets}) \\ &= C(n, 2m - o) \times C(2m - o, o) \times C(2m - 2o, m - o) \end{aligned}$$

These components allow us to compute $\text{cov}(EC_1, EC_2)$. However, to approximate the variance of EC_i over different subsamples, we will use the expectation of the variance estimator. Say we have taken B subsamples:

$$\begin{aligned} E[\text{v\hat{a}r}(EC_i)] &= E \left[\frac{1}{B} \sum_{i=1}^B (EC_i - \bar{EC})^2 \right] \\ &= E \left[\frac{1}{B} \sum_{i=1}^B EC_i^2 - \bar{EC}^2 \right] \\ &= E [EC_i^2] - E [\bar{EC}^2] \\ &= E [EC_i^2] - \frac{1}{B^2} E \left[\sum_{i=1}^B EC_i^2 + 2 \sum_{j < k} EC_j EC_k \right] \\ &= E [EC_i^2] - \frac{1}{B^2} \sum_{i=1}^B E [EC_i^2] - \frac{2}{B^2} \sum_{j < k} E [EC_j EC_k] \\ &= \frac{B-1}{B} E [EC_i^2] - \frac{2}{B^2} C(B, 2) E [EC_j EC_k] \\ &= \frac{B-1}{B} E [EC_i^2] - \frac{2}{B^2} \frac{B(B-1)}{2} E [EC_j EC_k] \\ &\approx E [EC_i^2] - E [EC_j EC_k] \\ &= E [EC_i^2] - E [EC_j] E [EC_k] - \text{cov}(EC_j, EC_k) \\ &= \text{var}(EC_i) - \text{cov}(EC_j, EC_k) \end{aligned}$$

Results:

α	0.05	0.1	0.15	0.2	0.25	0.3	0.5	0.6	0.7	0.8	0.9
$E_G [\text{KS}(F_1(G), F_c)]$ (naive)	0.0158	0.0317	0.0475	0.0633	0.0790	0.0947	0.1559	0.1855	0.2143	0.2422	0.2692
$E_G [\text{KS}(F_1(G), F_c)]$ (improved)	0.0158	0.0319	0.0482	0.0650	0.0821	0.0999	0.1792	0.2265	0.2824	0.3525	0.4517
$\hat{E}_G [\text{KS}(F_1(G), F_c)]$	0.0228	0.0383	0.0518	0.0690	0.0853	0.1033	0.1815	0.2284	0.2835	0.3532	0.4511

There is still some discrepancy, but it decreases as the proportion sampled increases. This is likely due to the normal approximation being poor when the number of nodes sampled is small.

Regardless of model, the form of B_o does not change, given uniform random sampling. For models under dyadic independence other than ER, the form of A_o changes due to different moments in terms $E[(e_j^1)^2]$ and $E[e_j^1]E[e_k^2]$ in the fifth line of the above expression for A_o . For example, with the weighted ER graph as formulated in Garlaschelli (2009), where each dyad is assigned weight W with geometric distribution:

$$\begin{aligned} P(W = w) &= p^w (1 - p) \\ P(\text{no edge}) &= P(W = 0) = 1 - p \\ P(\text{edge}) &= P(W > 0) = p \end{aligned}$$

Under this formulation:

$$\begin{aligned} E[(e_j^1)^2] &= \frac{p + p^2}{(1 - p)^2} \\ E[e_j^1] &= E[e_k^2] = \frac{p}{1 - p} \end{aligned}$$

For models not under dyadic independence, the $E[(e_j^1)^2]$ terms on the fifth line are still the second moment of an individual dyad, but all $E[e_j^1]E[e_k^2]$ terms must be replaced with $E[e_j^1 e_k^2]$ in order to properly account for dependence between dyads. The latter can be obtained from the covariance between dyads as specified by the model.

References

- W. Ali, A. E. Wegner, R. E. Gaunt, C. M. Deane, and G. Reinert. Comparison of large networks with sub-sampling strategies. *Scientific reports*, 6:28955, 2016.
- W. An. Fitting ergms on big networks. *Social science research*, 59:107–119, 2016.
- A.-L. Barabási and R. Albert. Emergence of scaling in random networks. *science*, 286(5439):509–512, 1999.
- J. Besag. Spatial interaction and the statistical analysis of lattice systems. *Journal of the Royal Statistical Society. Series B (Methodological)*, pages 192–236, 1974.
- S. Bhattacharyya, P. J. Bickel, et al. Subsampling bootstrap of count features of networks. *The Annals of Statistics*, 43(6):2384–2411, 2015.
- S. Chen, A. Mira, and J.-P. Onnela. Flexible model selection for mechanistic network models via super learner. *In progress*, 2018.
- C. Cooper and A. Frieze. A general model of web graphs. *Random Structures & Algorithms*, 22(3):311–335, 2003.
- B. A. Desmarais and S. J. Cranmer. Statistical mechanics of networks: Estimation and uncertainty. *Physica A: Statistical Mechanics and its Applications*, 391(4):1865–1876, 2012.
- B. Efron. Nonparametric estimates of standard error: the jackknife, the bootstrap and other methods. *Biometrika*, 68(3):589–599, 1981.
- P. Erdős and A. Rényi. On random graphs i. *Publ. Math. Debrecen*, 6:290–297, 1959.
- G. Fasano and A. Franceschini. A multidimensional version of the kolmogorov–smirnov test. *Monthly Notices of the Royal Astronomical Society*, 225(1):155–170, 1987.
- D. Garlaschelli. The weighted random graph model. *New Journal of Physics*, 11(7):073005, 2009.
- Y. R. Gel, V. Lyubchich, and L. L. R. Ramirez. Bootstrap quantification of estimation uncertainties in network degree distributions. *Scientific reports*, 7(1):5807, 2017.
- C. J. Geyer and E. A. Thompson. Constrained monte carlo maximum likelihood for dependent data. *Journal of the Royal Statistical Society. Series B (Methodological)*, pages 657–699, 1992.
- P. I. Good. *Resampling methods*. Springer, 2006.
- R. Goyal, J. Blitzstein, and V. De Gruttola. Sampling networks from their posterior predictive distribution. *Network Science*, 2(01):107–131, 2014.
- P. D. Hoff, A. E. Raftery, and M. S. Handcock. Latent space approaches to social network analysis. *Journal of the American Statistical Association*, 97(460):1090–1098, 2002.
- F. Hormozdiari, P. Berenbrink, N. Pržulj, and S. C. Sahinalp. Not all scale-free networks are born equal: the role of the seed graph in ppi network evolution. *PLoS computational biology*, 3(7):e118, 2007.
- D. R. Hunter, S. M. Goodreau, and M. S. Handcock. Goodness of fit of social network models. *Journal of the American Statistical Association*, 103(481):248–258, 2008.
- A. Justel, D. Peña, and R. Zamar. A multivariate kolmogorov-smirnov test of goodness of fit. *Statistics & Probability Letters*, 35(3):251–259, 1997.
- K. Klemm and V. M. Eguiluz. Highly clustered scale-free networks. *Physical Review E*, 65(3):036123, 2002.
- J. M. Kumpula, J.-P. Onnela, J. Saramäki, K. Kaski, and J. Kertész. Emergence of communities in weighted networks. *Physical review letters*, 99(22):228701, 2007.

- S. Li, K. P. Choi, and T. Wu. Degree distribution of large networks generated by the partial duplication model. *Theoretical Computer Science*, 476:94–108, 2013.
- D. Lusher, J. Koskinen, and G. Robins. *Exponential random graph models for social networks: Theory, methods, and applications*. Cambridge University Press, 2013.
- M. Newman. *Networks: an introduction*, 2010.
- K. Ohara, K. Saito, M. Kimura, and H. Motoda. Resampling-based framework for estimating node centrality of large social network. In *International Conference on Discovery Science*, pages 228–239. Springer, 2014.
- R. Pastor-Satorras and A. Vespignani. *Evolution and structure of the Internet: A statistical physics approach*. Cambridge University Press, 2007.
- R. Pastor-Satorras, E. Smith, and R. V. Solé. Evolving protein interaction networks through gene duplication. *Journal of Theoretical Biology*, 222(2):199–210, 2003.
- J. Peacock. Two-dimensional goodness-of-fit testing in astronomy. *Monthly Notices of the Royal Astronomical Society*, 202(3):615–627, 1983.
- E. C. Polley, S. Rose, and M. J. Van der Laan. Super learning. In *Targeted Learning*, pages 43–66. Springer, 2011.
- A. Raval and A. Ray. *Introduction to biological networks*. CRC Press, 2013.
- G. Robins, P. Pattison, Y. Kalish, and D. Lusher. An introduction to exponential random graph (p^*) models for social networks. *Social networks*, 29(2):173–191, 2007.
- L. Salwinski, C. S. Miller, A. J. Smith, F. K. Pettit, J. U. Bowie, and D. Eisenberg. The database of interacting proteins: 2004 update. *Nucleic acids research*, 32(suppl_1):D449–D451, 2004.
- R. Schweiger, M. Linial, and N. Linial. Generative probabilistic models for protein-protein interaction networks—the biclique perspective. *Bioinformatics*, 27(13):i142–i148, 2011.
- J. Shore and B. Lubin. Spectral goodness of fit for network models. *Social Networks*, 43:16–27, 2015.
- T. A. Snijders. Markov chain monte carlo estimation of exponential random graph models. *Journal of Social Structure*, 3(2):1–40, 2002.
- R. V. Solé, R. Pastor-Satorras, E. Smith, and T. B. Kepler. A model of large-scale proteome evolution. *Advances in Complex Systems*, 5(01):43–54, 2002.
- M. E. Thompson, L. L. Ramirez Ramirez, V. Lyubchich, and Y. R. Gel. Using the bootstrap for statistical inference on random graphs. *Canadian Journal of Statistics*, 44(1):3–24, 2016.
- M. J. Van der Laan, E. C. Polley, and A. E. Hubbard. Super learner. *Statistical applications in genetics and molecular biology*, 6(1), 2007.
- M. A. Van Duijn, K. J. Gile, and M. S. Handcock. A framework for the comparison of maximum pseudo-likelihood and maximum likelihood estimation of exponential family random graph models. *Social Networks*, 31(1):52–62, 2009.
- A. Vázquez, A. Flammini, A. Maritan, and A. Vespignani. Modeling of protein interaction networks. *Complexus*, 1(1):38–44, 2003.
- S. Wasserman and K. Faust. *Social network analysis: Methods and applications*, volume 8. Cambridge university press, 1994.
- D. J. Watts. *Six degrees: The science of a connected age*. WW Norton & Company, 2004.
- D. J. Watts and S. H. Strogatz. Collective dynamics of ‘small-world’ networks. *nature*, 393(6684):440–442, 1998.
- C.-F. J. Wu. Jackknife, bootstrap and other resampling methods in regression analysis. *the Annals of Statistics*, pages 1261–1295, 1986.